LTD-inducing low frequency stimulation enhances p-Tau181 and p-Tau217 in an age-dependent manner in live rats

Running head: LTD elevates p-Tau181/217 in aged rats

Yangyang Zhang[1,#], Yin Yang[1,#], Zhengtao Hu[1,2,#], Manyi Zhu[1], Shuangying Qin[1], Pengpeng Yu[1,3], Bo Li[1], Jitian Xu[1], Michael J. Rowan[3] and Neng-Wei Hu[1,3,*]

[1]Department of Physiology and Neurobiology, School of Basic Medical Sciences, Zhengzhou University, 100 Science Avenue, Zhengzhou 450001, China

[2]Department of Gerontology, The First Affiliated Hospital of Wannan Medical College, Wuhu 241001, China

[3]Department of Pharmacology & Therapeutics and Institute of Neuroscience, Trinity College, Dublin 2, Ireland

[#]These authors contributed equally to this work.

*Correspondence to Neng-Wei Hu, E-mail: hunw@tcd.ie

Abbreviations:

AD: Alzheimer's disease

Aβ: amyloid-β protein

$A\beta_{O:}$ Aβ oligomers

CSF: cerebrospinal fluid

Cdk5: cyclin-dependent kinase-5

DAPI: 4′,6-diamidino-2-phenylindole

DG: dentate gyrus

DMSO: dimethyl sulfoxide

EPSP: excitatory postsynaptic potential

GSK3α: glycogen synthase kinase 3α

GSK3β: glycogen synthase kinase 3β

HFS: high frequency stimulation

i.c.v.: intracerebroventricular

ISR: integrated stress response

LFS: low frequency stimulation

LTD: long-term depression

LTP: long-term potentiation

mGluR5: metabotropic glutamate receptor subtype 5

NMDA: N-methyl-D-aspartate

NMDAR: N-methyl-D-aspartate receptor

PEG400: polyethylene glycol 400

PMSF: phenylmethylsulfonyl fluoride

PrP^{C}: cellular prion protein

PVDF: polyvinylidene fluoride

p-Tau: phosphorylated tau

SDS: sodium dodecyl sulfate

TBS-T: tris-buffered saline containing 0.1% Tween 20

Abstract

The progressive cognitive decline in Alzheimer's disease (AD) patients correlates with the extent of tau pathology, in particular tau hyperphosphorylation, which is strongly age-associated. Although elevation of phosphorylated tau (p-Tau) on residues Thr181 (p-Tau181), Thr217 (p-Tau217), and Thr231 (p-Tau231) in cerebrospinal fluid or blood are recently proposed to be particularly sensitive markers of early AD, the generation of p-Tau during brain activity is poorly understood. A major form of synaptic plasticity, long-term depression (LTD), has recently been linked to the enhancement of tau phosphorylation. Here we show that low frequency stimulation (LFS), used to induce LTD, enhances p-Tau181 and p-Tau217 in an age-dependent manner in the hippocampus of live rats. In contrast, phosphorylation at residues Thr231, Ser202/Thr205, and Ser396 is less sensitive to LFS. Pharmacological antagonism of either NMDA or metabotropic glutamate 5 (mGluR5) receptors inhibits the elevation of both p-Tau181 and p-Tau217. Targeting ageing with a small molecule cognitive enhancer ISRIB (trans-isomer) prevents the enhancement of p-Tau by LFS in aged rats. Together, our data provide an *in vivo* means to uncover brain plasticity-related cellular and molecular processes of tau phosphorylation in health and ageing conditions.

Key words:

ageing / long-term depression / synaptic plasticity / tau phosphorylation

Introduction

Clinical evidence indicates that age-associated progressive cognitive decline in Alzheimer's disease (AD) patients correlates with the extent of tau pathology, in particular the degree and nature of tau phosphorylation (Chang *et al*, 2021; Nies *et al*, 2021; Wegmann *et al*, 2019; Wesseling *et al*, 2020). Among the latter, elevation of phosphorylated tau (p-Tau) on residues of Thr181 (p-Tau181), Thr217 (p-Tau217), and Thr231 (p-Tau231) in cerebrospinal fluid (CSF) or blood were recently proposed to be particularly sensitive markers of early AD, long before the diagnosis of clinical dementia (Barthelemy *et al*, 2020a; Barthelemy *et al*, 2020b; Hansson, 2021; Karikari *et al*, 2020; O'Connor *et al*, 2020; Palmqvist *et al*, 2021; Wegmann *et al*, 2021). P-Tau in the brain and its subsequent release into CSF and blood is a dynamic process that changes during disease evolution. Although reports from various memory clinics indicate that p-Tau181, p-Tau217, and p-Tau231 distinguish AD from controls with high accuracy for very early AD diagnosis, the generation of these p-Tau species in patients' brains, in particular learning and memory processes, is still unclear, mainly due to ethical and technical limitations.

The hippocampus is one of the areas that p-Tau first appears during Braak stage II of AD (Braak *et al*, 2006) and this region of brain is particularly vulnerable to age-related changes (Buss *et al*, 2021; Driscoll *et al*, 2003; Ianov *et al*, 2017; McKiernan & Marrone, 2017; Veldsman *et al*, 2021). Synaptic plasticity mechanisms at excitatory glutamatergic synapses in hippocampus, including those underlying long-term depression (LTD), are neurophysiological substrates of normal learning and

memory function (Connor & Wang, 2016; Magee & Grienberger, 2020). Interestingly, recent studies indicate that LTD induction enhances tau phosphorylation at Ser396 (p-Tau396) (Kimura *et al*, 2014; Regan *et al*, 2015) and Ser202/Thr205 (p-Tau202/205) (Taylor *et al*, 2021) in hippocampus *in vitro*. It is still unknown whether the expression levels of p-Tau181, p-Tau217, and p-Tau231 can also be enhanced by physiological LTD induction. Whether or not their enhancement is more sensitive compared with other reported residues and the age-dependence of tau phosphorylation remains elusive.

Both NMDAR and metabotropic glutamate receptors are required for the induction of most forms of LTD by low frequency conditioning stimulation (LFS) (Collingridge *et al*, 2010). Recent evidence implicates a particular role for extrasynaptic NMDAR (Liu *et al*, 2013; Papouin *et al*, 2012) and metabotropic glutamate receptor subtype 5 (mGluR5) (Hu *et al*, 2014; Li *et al*, 2009; Luscher & Huber, 2010; O'Riordan *et al*, 2018a), both also involved in tau pathology (Benarroch, 2018; Sun *et al*, 2016; Tackenberg *et al*, 2013), in LTD induction.

Here we investigated whether p-Tau181, p-Tau217, p-Tau231, p-Tau202/205 and p-Tau396 are affected by the induction of hippocampal LTD by LFS at CA3 to CA1 synapses in the hippocampus of live rats (Hu *et al.*, 2014; O'Riordan *et al*, 2018b; Ondrejcak *et al*, 2019). We assayed the local expression of p-Tau in different subregions of hippocampus at two different ages (2-3-months and 17-18-months). We found that electrical LFS preferentially enhanced p-Tau181 and p-Tau217 in an age-dependent manner without apparently affecting the levels of p-Tau at other

residues that were investigated. Further, blocking either NMDARs or mGluR5 with their selective antagonists strongly inhibited the elevation of both p-Tau181 and p-Tau217. Finally, targeting ageing with ISRIB (trans-isomer) (Krukowski *et al*, 2020) prevented the increase of both p-Tau181 and p-Tau217 by LFS in aged rats. Our data provide an *in vivo* means to uncover brain plasticity-related cellular and molecular processes of tau phosphorylation in health and disease.

Results

Induction of LTD by LFS enhances p-Tau181, p-Tau217 in an age-dependent manner in live rats

Pyramidal neurons in hippocampal CA1 area is one of the fields that p-Tau first appears during Braak stage II of AD (Braak *et al.*, 2006). Although LFS-triggered tau phosphorylation at Ser396 (Kimura *et al.*, 2014; Regan *et al.*, 2015) and Ser202/Thr205 (Taylor *et al.*, 2021) in hippocampal slices has been previously reported, the effects of LTD-inducing LFS on the expression of p-Tau181, p-Tau217, and p-Tau231, recently proposed to be particularly sensitive markers of early AD, have yet to be described. Having developed stimulation protocols to reliably induce LTD at CA3 to CA1 synapses in live rats (Hu *et al.*, 2014; O'Riordan *et al.*, 2018a, b; Ondrejcak *et al.*, 2019), we confirmed (Hu *et al.*, 2014) that this protocol (LFS-900, 900 pulses at 1 Hz) triggered a robust persistent form of LTD that, like certain forms of long-term memory formation, is protein synthesis-dependent (**Figure S1**). We used the same protocol (LFS-900, 900 pulses at 1 Hz) in this study (**Figure 1a**). To determine the age-dependence of p-Tau enhancement by LFS, we performed our

experiments in rats at two different ages: 2-3 months and 17-18 months. LFS depressed field EPSPs to 63.8 ± 7.8% of baseline in 2-3-month-old rats, and 62.4 ± 3.4% in 17-18-month-old rats. The magnitude of LFS-induced synaptic depression is thus comparable at both ages (**Figure 1b,c**).

The rats were sacrificed 30 min post-LFS and immunohistochemically processed for p-Tau181, p-Tau217, p-Tau231, p-Tau202/205, p-Tau396, and total tau analysis (all antibodies used are in **Table S1** and in the Methods). The expression level of total tau and p-Tau was measured in whole dorsal hippocampus, CA1, CA3, and the hilus of dentate gyrus (DG in this study) areas. The expression level in the contralateral hemisphere was used as the control. Immunofluorescent staining for antibody Tau46 or Tau5 confirmed that application of LFS did not lead to a change in total tau expression level in both age groups (**Figure S2**). Whereas no difference of p-Tau181 level was apparent in 2-3-month-old (**Figure 1d**), in 17-18-month-old animals tau phosphorylation at Thr181 was obviously enhanced in all three hippocampal fields (**Figure 1e**). We then assayed the expression level of p-Tau217 in adjacent brain slices from the same animals. Similar to p-Tau181, no difference was observed in 2-3-month-old rats (**Figure 2a**), while an enhancement of p-Tau217 was seen in CA1, CA3, and DG in 17-18-month-old rats (**Figure 2b**). In contrast, the expression levels of p-Tau231, p-Tau202/205 and p-Tau396 did not appear to change in adjacent brain slices from young (**Figure S3**) or aged rats overall, with the exception of a significant enhancement of p-Tau202/205 in the CA1 area of older rats (**Figure S4**).

To determine if the changes in p-Tau by LTD-inducing LFS detected using

immunohistochemistry referenced to the contralateral hemisphere, we measured the expression level of the same phospho-tau species using western blotting after the same conditioning LFS was applied in another cohort of 17-18-month-old rats (**Figure 3a,b**). β-actin was used to ensure equal protein loading on gels. The total tau expression level, normalized to β-actin, in either the ipsilateral or contralateral hippocampus did not differ from age-matched naïve control rats (**Figure S5**). Consistent with the immunohistochemistry, LTD-inducing LFS significantly enhanced p-Tau181 (**Figure 3c**; **Figure S6**) and p-Tau217 (**Figure 3d**; **Figure S6**) in the ipsilateral hippocampus, while it had no overall significant effect compared with naïve controls on the expression level of p-Tau at the other residues investigated (**Figure S7**). Western blotting indicated that the expression levels of p-Tau181 and p-Tau217, slightly, although not significantly, also increased in the contralateral hippocampus when compared with naïve controls. This indicates that application of LFS activates the commissural pathway sufficiently to enhance the expression levels of both p-Tau181 and p-Tau217 in parts of the contralateral hippocampus.

Enhanced neuronal activity accelerates tauopathy *in vivo* in tau mouse models (Wu *et al*, 2016) and mechanical injury of neurons induces tau mislocalization to dendritic spines (Braun *et al*, 2020). In order to exclude any influence of electrode implantation and baseline recording of evoked field EPSPs on the local expression level of p-Tau, the same experimental processes were performed but no LFS was applied in another cohort of 17-18-month-old rats (**Figure S8a,b**). The immunofluorescent staining results confirmed that no change of p-Tau181 and p-Tau217 levels were present in

hippocampus from these rats (**Figure S8c,d**). We thus demonstrate that application of LFS enhances p-Tau181 and p-Tau217 in an age-dependent manner in live rats. The enhancement of tau phosphorylation at both residues by LFS appears more sensitive compared with residues Thr231, Ser202/Thr205, and Ser396.

Antagonists of NMDA receptors or mGluR5 inhibit the elevation of both p-Tau181 and p-Tau217

Previously, we found that the induction of LTD by LFS, was not blocked by standard systemic doses of either NMDAR or mGluR5 antagonists when applied alone (Hu *et al.*, 2014; O'Riordan *et al.*, 2018b), while combined systemic injection of both antagonists completely abrogated the induction of synaptic LTD in young adult rats (O'Riordan *et al.*, 2018b). Therefore, we wondered if synaptic LTD could be blocked by standard systemic doses of either NMDAR or mGluR5 antagonists when applied alone in relatively aged (17-18-month-old) rats. Similar to our previous finding in young rats (Hu *et al.*, 2014; O'Riordan *et al.*, 2018b), a standard systemic dose (10 mg/kg, i.p.) of the competitive NMDAR antagonist CPP which completely blocked synaptic long-term potentiation (LTP) in CA3-CA1 synapses (**Figure S9**), did not affect the induction of LTD in aged rats. Thus 1 h post the injection of CPP, the application of LFS suppressed the field EPSPs to 70.2 ± 2.5% in 17-18-month-old rats (**Figure 4a,b**). Next we tested the standard dose of MTEP (3 mg/kg, i.p.) which is known to non-competitively block mGluR5, with a rat hippocampal receptor occupancy of > 90% (Busse *et al*, 2004). The application of LFS induced a depression of field EPSPs to 79.6 ± 3.7% in these MTEP-treated animals (**Figure 4a,b**).

Given that neither block of NMDAR with CPP nor block of mGluR5 with MTEP prevented the induction of LTD in aged rats, we hypothesized that neither of these treatments on their own would affect the enhancement of p-Tau181 and p-Tau217 by LFS. To test this, we assessed total tau and p-Tau on both residues in the hippocampus of the rats treated with CPP or MTEP. Immunofluorescent staining for antibody Tau46 confirmed that neither agent affected total tau expression level after induction of LTD by LFS in aged rats (**Figure S10**). Surprisingly, even though neither of these treatments on their own affected the induction of LTD, elevation of p-Tau181 and p-Tau217 by LFS were abolished/inhibited in both CPP and MTEP-treated aged rats. After systemic treatment of CPP, the enhancement of p-Tau181 by LFS was strongly inhibited overall although some enhancement was seen in the CA1 area (**Figure 4c**), while the elevation of p-Tau217 by LFS was completely abolished (**Figure 4d**). Somewhat similarly, the elevation of both p-Tau181 and p-Tau217 triggered by LFS was completely prevented by systemic administration of MTEP (**Figure 4e,f**). CPP is a competitive NMDAR antagonist, so its ability to block NMDARs depends on the magnitude of stimulus-evoked transmitter release during the LFS period. This may help explain why the enhancement of p-Tau181 was resistant to CPP in the CA1 area. Together, these findings indicate that increases of p-Tau181 and p-Tau217 triggered by LFS needs the co-activation of mGluR5 and NMDARs.

Targeting ageing with a small molecule cognitive enhancer ISRIB blocks the enhancement of p-Tau181 and p-Tau217 by LFS in aged rats

Given that induction of LTD by LFS enhances p-Tau181 and p-Tau217 in an

age-dependent manner and ageing is the greatest risk factor for AD (Hou *et al*, 2019), we hypothesized that targeting ageing might prevent the elevation of p-Tau181 and p-Tau217 by LFS. Very recently, Krukowski et al. discovered that the small molecule cognitive enhancer ISRIB reverses age-associated changes in hippocampal neuron function (Krukowski *et al.*, 2020). To test this hypothesis, we treated relatively aged (17-18-month-old) rats with the same ISRIB treatment paradigm of daily injections on 3 consecutive days as reported (Krukowski *et al.*, 2020), and *in vivo* electrophysiological experiments were carried out on these animals 18 days after the last injection of ISRIB (**Figure 5a**). LFS induced stable and robust LTD in all these rats (**Figure 5b,c**). Immunofluorescent staining for antibody Tau46 confirmed that induction of LTD by LFS did not lead to a change in total tau expression level in ISRIB-treated rats (**Figure S11**). Intriguingly, neither p-Tau181 (**Figure 5d**) nor p-Tau217 (**Figure 5e**) were increased by the same LFS conditioning protocol which triggered enhancement of both p-Tau181 and p-Tau217 in untreated age-matched rats (**Figure 1e** and **Figure 2b**).

Discussion

This study reveals that ageing enables the elevation of p-Tau181 and p-Tau217 triggered by LTD-inducing conditioning stimulation in live rats. Growing evidence from many different memory center cohorts indicates that p-Tau181 and p-Tau217 distinguish AD from controls with high accuracy very early in the disease process (Hansson, 2021; Teunissen *et al*, 2022). These findings encourage the prospect that these markers are good enough to become early AD diagnostic tools. Our data provide

a novel *in vivo* means to uncover brain plasticity-related cellular and molecular processes of tau phosphorylation at these key sites in health and ageing.

Because LTD induction by LFS at CA3-CA1 synapses in the hippocampus usually necessitates transient elevated synaptic glutamate release and subsequent activation of NMDARs and/or mGluRs (Collingridge *et al.*, 2010), we wondered if the enhanced tau phosphorylation triggered by LFS entails these receptors also. Pretreatment with either the NMDAR or mGluR5 antagonist alone completely abrogated the LFS-induced tau phosphorylation, indicating that both receptors need to be activated to trigger enhanced p-Tau181 and p-Tau217. Although we only examined one time point, it is clear that LFS triggers an NMDAR and mGluR5-dependent increase in tau phosphorylation that persists for at least 30 min in all hippocampal subfields examined. Whereas the induction of *in vivo* LTD is only blocked by combined pretreatment with standard doses of CPP and MTEP (O'Riordan *et al.*, 2018b), injecting either agent alone (Hu *et al.*, 2014; O'Riordan *et al.*, 2018b) prevented LFS-triggered tau phosphorylation. In view of these findings, it seems unlikely that enhanced tau phosphorylation at either residues Thr181 or Thr217 is essential for LTD at CA3-CA1 synapses. Also, it remains to be determined if the LFS protocol used in the present study triggers LTD at CA3 recurrent collaterals or back projections as reported previously (Debanne *et al*, 1998). Recent evidence implicates a particular role for extrasynaptic NMDAR in LTD induction (Liu *et al.*, 2013; Papouin *et al.*, 2012). In the hippocampal CA1 area, mGluR5 is found predominantly located perisynaptically and extrasynaptically on postsynaptic spines of pyramidal

cells (Lujan *et al*, 1996; Lujan *et al*, 1997). Co-activation of mGluR5 with NMDARs located in this vicinity is known to strongly enhance the function of the NMDARs, in particular GluN2B-containing NMDARs (Kotecha *et al*, 2003; Sarantis *et al*, 2015). Numerous studies have shown that synaptic NMDARs are mainly involved in normal cognitive function, while extrasynaptic NMDARs are important mediators of neurotoxicity (Vieira *et al*, 2020). Glutamate-induced excitotoxicity increases tau phosphorylation (Sindou *et al*, 1994) and more recent evidence indicates the involvement of extrasynaptic NMDARs activation in tau pathology (Sun *et al.*, 2016; Tackenberg *et al.*, 2013). Tau is phosphorylated at many different sites by different protein kinases. Both glycogen synthase kinase 3β (GSK3β) and cyclin-dependent kinase-5 (Cdk5) can phosphorylate tau at Thr181 and Thr217 (Liu *et al*, 2002). The activity of GSK3β is significantly enhanced during hippocampal LTD (Peineau *et al*, 2007) but very recent evidence indicates the involvement of GSK3α in both NMDAR-dependent (Draffin *et al*, 2021) and mGluR5-dependent (McCamphill *et al*, 2020) LTD. Cdk5 activation appears to be required for NMDAR-dependent LTD at CA3-CA1 synapses also (Mishiba *et al*, 2014).

Ageing is the primary risk factor for most neurodegenerative diseases including AD (Hou *et al.*, 2019). Age-related reduction in glutamate uptake is associated with extrasynaptic NMDAR and mGluR activation at hippocampal CA1 synapses (Potier *et al*, 2010). Very recent evidence indicates that imbalanced synaptic weights undies the aberrant elevated firing characteristics of both CA3 and CA1 pyramidal neurons in aged, learning impaired rats (Buss *et al.*, 2021). Intriguingly, Krukowski et al.

295 discovered that a small molecule cognitive enhancer ISRIB reverses the aberrantly
296 elevated integrated stress response (ISR) in aged mice brain and restores age-related
297 changes in hippocampal neuron function (Krukowski *et al.*, 2020). In the present
298 study, the same ISRIB treatment paradigm successfully prevented the elevation of
299 both p-Tau181 and p-Tau217 by LFS in aged rats. Although the detailed mechanisms
300 of how ISRIB prevents tau phosphorylation remain to be elucidated, given that ageing
301 is the single strongest risk factor for AD, targeting ageing is likely to provide novel
302 therapeutic avenues for AD (Livingston *et al*, 2020).
303 Previous reports indicate that p-Tau396 can be enhanced by LFS-900 (1 Hz) in acute
304 hippocampal slices (Kimura *et al.*, 2014; Regan *et al.*, 2015). In contrast, no change in
305 p-Tau202/205 was triggered by LFS except under the extreme condition of 2 hours
306 LTD induction over a period of 7 days in slice cultures (Taylor *et al.*, 2021). The
307 experimental conditions used to detect changes in p-Tau396 in hippocampal slices
308 differ very significantly from our live brain studies, including relatively young age
309 and non-physiological temperature. It is well recognized that p-Tau is
310 developmentally regulated (Bramblett *et al*, 1993; Brion *et al*, 1993; Goedert *et al*,
311 1993; Hefti *et al*, 2019; Yu *et al*, 2009) and can be hypothermia-induced (Avila &
312 Diaz-Nido, 2004; Bretteville *et al*, 2012; Gratuze *et al*, 2017; Planel *et al*, 2004).
313 Although not statistically significant, we found slight elevation of p-Tau396 triggered
314 by LFS-900 *in vivo* in this study. Nevertheless, future studies should elucidate if, like
315 the present *in vivo* studies, changes in p-Tau181 and p-Tau217 are more sensitive to
316 LTD-inducing LFS *in vitro*. Phosphorylated tau species have faster tau turnover rates

and shorter half-lives in cultured human and rodent neurons compared with that in human and rodent brains (Sato *et al*, 2018). Thus, our findings in live animals provide a valuable experimental model to directly study the generation of p-Tau during learning and memory-related synaptic plasticity and to help develop clinical biomarkers of AD.

Further highlighting that AD is a chronic disease, it is feasible to carry out more detailed time course analysis of phosphorylated tau in our live animal models. To conclude, our data in this study show that, similar to clinical biomarker findings, tau phosphorylation is preferentially triggered at certain sites including Thr181 and Thr217 by LTD-inducing conditioning stimulation in aged brain in live rats. Given current technical and ethical barriers to tau detection in live patient's brain, our experimental models provide a valuable means to (1) directly study the generation of p-Tau during learning and memory-related synaptic plasticity, (2) help optimize the choice of p-Tau as biomarkers, and (3) aid in the selection of p-Tau directed therapies in future clinical trials of AD.

Materials and Methods

Animals

All experiments were performed following the guidelines of the ARRIVE (Animal Research: Reporting of In Vivo Experiments) guidelines 2.0 (Percie du Sert *et al*, 2020) and were approved by the Animal Care and Use Committee of Zhengzhou University, China. All efforts were made to minimize the number of animals used and their suffering.

Young adult (2-3-month-old), and aged (17-18-month-old) male Sprague Dawley rats were provided by the Laboratory Animal Center of Zhengzhou University. The animals were housed under a 12 h light-dark cycle at room temperature (19-22^{o}C) with continuous access to food and water *ad libitum*. Prior to the acute experiments, animals were anaesthetized with urethane (1.5-1.6 g/kg, i.p.). Lignocaine (10 mg, 1% adrenaline, s.c.) was injected over the area of the skull where electrodes and screws were to be implanted. The body temperature of the rats was maintained at 37-38^{o}C with a feedback-controlled heating blanket during the whole period of surgery and recording.

Electrophysiology

Electrodes were made and implanted as described previously (Hu *et al.*, 2014). Briefly, monopolar recording electrodes were constructed from Teflon-coated tungsten wires (75 μm inner core diameter, 112 μm external diameter) and twisted bipolar stimulating electrodes were constructed from Teflon-coated tungsten wires (50 μm inner core diameter, 75 μm external diameter) separately. Field excitatory postsynaptic potentials (EPSPs) were recorded from the stratum radiatum in the CA1 area of left or right hippocampus in response to stimulation of the Schaffer collateral-commissural pathway. Electrode implantation sites were identified using stereotaxic coordinates relative to bregma, with the recording site located 3.4 mm posterior to bregma and 2.5 mm lateral to midline, and stimulating site 4.2 mm posterior to bregma and 3.8 mm lateral to midline. The final placement of electrodes was optimized by using electrophysiological criteria and confirmed via postmortem

analysis.

Test EPSPs were evoked by a single square wave pulse (0.2 ms duration) at a frequency of 0.033 Hz and an intensity that triggered a 50% maximum EPSP response. LTD was induced using 1 Hz low frequency stimulation (LFS) consisting of 900 pulses (0.2 ms duration). During the LFS the intensity was raised to trigger EPSPs of 95% maximum amplitude. LTP was induced using 200 Hz high frequency stimulation (HFS) consisting of one set of 10 trains of 20 pulses (inter-train interval of 2 s). The stimulation intensity was raised to trigger EPSPs of 75% maximum during the HFS. None of the conditioning stimulation protocols elicited any detectible abnormal changes in background EEG, which was recorded from the hippocampus throughout the experiments.

Immunofluorescent staining

After electrophysiological recording under anesthesia of urethane, rats were transcardially perfused with pre-warmed normal saline followed by cold 4% paraformaldehyde in PBS at pH 7.4. Brains were carefully removed and post-fixed in 4% paraformaldehyde for 6 h. Brains were dehydrated in 20% sucrose followed by 30% sucrose. Tissues were rapidly frozen and cut coronally (50 μm). Sections near the stimulating and recording electrodes were reserved and stored in cryoprotective solution (150 mM ethylene, 100 mM glycerol, 250 mM PBS) at -20°C. For total tau and phosphorylated-tau staining, sections were washed three times with PBS for 5 min and then permeabilized with 0.1% Triton X-100 diluted in PBS for 30 min at room temperature. Then sections were blocked in a PBS solution containing 10%

normal goat serum, 3% BSA, 0.1% Triton X-100 for 1 h at room temperature. Sections were incubated respectively with the primary antibodies (**Table S1**) (Tau5, Cell Signaling Technology, 46687S, 1:200; Tau46, Cell Signaling Technology, 4019S, 1:200; Phospho-Tau (Thr181), Cell Signaling Technology, 12885S, 1:200; Phospho-Tau (Thr217), ThermoFisher, 44-744, 1:200; Phospho-Tau (Thr231), Abcam, ab151559, 1:200; Phospho-Tau (Ser202, Thr205), ThermoFisher, MN1020, 1:200; Phospho-Tau (Ser396), Affinty, AF3148, 1:200) in a humidified chamber overnight at 4°C. After 24 h, sections were washed three times with PBS for 5 min, followed by incubation with species-specific secondary antibodies conjugated to 488 nm or 568 nm fluorophores (Alexa Fluor® 488, Abcam, 150113, 1:500; Alexa Fluor® 568, Abcam, 175471, 1;500) for 1 h at room temperature. Sections were subsequently washed and stained with DAPI solution (Solarbio, C0065) for 10 min at room temperature. After washing with PBS, sections were mounted on the glass slide with antifade mountant (Southern Biotech, 0100-20) and then processed for imaging using an Olympus fluorescent microscope (BX5WI, Olympus, Japan). ImageJ version 1.52a software (National Institute of Mental Health, Bethesda, Maryland, USA) was used to analyze the intensity of total tau, p-Tau of immunofluorescent staining.

Western blot

The rats were sacrificed 30 min post-LFS in the LFS-treated group or the same timeline under urethane anaesthesia in the naïve control group. The whole brain was taken out and the hippocampus from both sides was separated. Approximately 2-mm-thick hippocampal tissue surrounding the sites of electrodes was kept and

frozen immediately in liquid nitrogen and stored at -80°C. The tissues were homogenized in lysis buffer (10mM Tris-HCl, pH 7.5, 150mM NaCl, and 0.5% Triton X-100, 0.1mM PMSF) containing 1% protease inhibitor Cocktail (Sigma-Aldrich, CW2200S) and 1% phosphatase inhibitor Cocktail (Sigma-Aldrich, CW2383S). The protein concentrations were determined by the BCA Protein Assay Kit (Glpbio, GK10009), and samples were separated by 10% Tris-glycine SDS-PAGE. The proteins were transferred onto polyvinylidene fluoride (PVDF) membranes (Millipore, IPVH00010). Then the membranes were blocked with 5% non-fat milk for 1 h at room temperature. After blocking, the membranes were incubated respectively with the primary antibodies (**Table S1**) overnight at 4°C. After primary antibody incubation, the membranes were washed three times in TBST and then incubated with HRP-conjugated goat anti-rabbit IgG (ZSGB-BIO, ZB-2301, 1:25000) for 2 h at room temperature. Finally, the target protein bands were visualized with chemiluminescence reagents (Shanghai Willget Biotech, F03) and then detected with ProteinSimple System (Hybrid HY8300, FluorChem E system, USA). Quantification of the protein expression was calculated with ImageJ (version 1.52a).

Pharmacological agents

(R,S)-3-(2-carboxypiperazin-4-yl)propyl-1-phosphonic acid ((±)-CPP, Alomone, C-175) and 3-((2-methyl-1,3-thiazol-4-yl)ethynyl)pyridine hydrochloride (MTEP hydrochloride, Abcam, ab120035) were prepared in distilled water and diluted with saline to the required concentration.

Trans-N,N′-(Cyclohexane-1,4-diyl)bis(2-(4-chlorophenoxy) acetamide (ISRIB,

Sigma, SML0843) was dissolved in dimethyl sulfoxide (DMSO) with gentle warming in a 40^{o}C water bath and vortexed until the solution became clear. Then the solution was diluted in polyethylene glycol 400 (PEG400) with gentle warming in a 40^{o}C water bath and vortexed. The solution was prepared freshly and diluted in warm saline (37^{o}C) before injection. 1:1 DMSO and PEG400 in saline was used as vehicle control. The choice of dose and timing of ISRIB administration was based on previous reports (Krukowski *et al.*, 2020) and our study of the pharmacokinetics of ISRIB in live rats (Hu *et al*, 2022). Four pair-housed relatively aged (17-18-month-old) rats received a single daily injection of ISRIB (2.5 mg/kg, i.p.) on 3 consecutive days. Then the rats stayed pair-housed for 18 days after the third injection of ISRIB.

Data analysis

Values are expressed as the mean ± s.e.m. For the electrophysiology experiments, the last 10 min prior to LFS was used to calculate the "Pre" -induction EPSP amplitude. Unless otherwise stated the magnitude of LTD was measured over the last 10 min at the end of recording after ("Post") LFS. To compare between two group, repeated measures two-way ANOVA with Bonferroni *post hoc* test was used. To compare between groups of three or more, one-way ANOVA with Bonferroni multiple comparisons was used. A two-tailed paired Student's *t*-test (paired *t*) was used to compare between "Pre" and "Post" within groups. For the immunofluorescence staining, internal comparison was used. Thus, immunofluorescent staining signal was quantified in the entire and selected subregions of the ipsilaterally stimulated hippocampi and the contralateral one from the same animals. The average of the

449 contralateral control was standardized to 1. A two-tailed paired Student's *t*-test was
450 used to compare between ipsilateral and contralateral. Data of western blotting
451 between conditions were compared using one-way ANOVA with Bonferroni multiple
452 comparisons. A value of $P < 0.05$ was considered statistically significant (*$P < 0.05$,
453 **$P < 0.01$, ***$P < 0.001$, ****$P < 0.0001$). All data were evaluated and graphed
454 using Prism 9.0 (GraphPad Inc, San Diego, CA, USA).

455 **Data availability**

456 All raw data supporting the findings of this study are available from the
457 corresponding author upon reasonable request.

458 **Acknowledgments**

459 This study has been funded by National Natural Science Foundation of China
460 (U2004134) and Zhengzhou University (140/32310295) to NWH, and by Science
461 Foundation Ireland (19/FFP/6437 and 14/IA/2571) to MJR. The funders had no role
462 in study design, data collection and analysis, decision to publish, or preparation of the
463 manuscript. We thank Professor Seán Kennelly (Tallaght University Hospital, Trinity
464 College Dublin) and Professor Tim Lynch (Mater Misericordiae University Hospital,
465 University College Dublin) for advice.

466 **Author contributions**

467 NWH and MJR jointly conceptualized the study and NWH directed experiments; YZ,
468 ZH, and PY conducted the electrophysiological experiments; YZ, YY, MZ, and SQ
469 performed immunofluorescent staining; YZ, YY, MZ, and SQ performed Western blot;
470 BL and JX assisted with Western blot and immunofluorescent staining; All authors

contributed to preparing figures and data analysis; NWH wrote the first draft of the manuscript; All authors contributed to reviewing and editing the manuscript, and approved its final version.

Conflict of interest

The authors have no competing interests to declare that are relevant to the content of this article.

Ethics approval

All experiments were performed following the guidelines of the ARRIVE (Animal Research: Reporting of In Vivo Experiments) guidelines 2.0 (Percie du Sert *et al.*, 2020) and were approved by the Animal Care and Use Committee of Zhengzhou University, China. All efforts were made to minimize the number of animals used and their suffering.

References

Avila J, Diaz-Nido J (2004) Tangling with hypothermia. *Nat Med* 10: 460-461

Barthelemy NR, Horie K, Sato C, Bateman RJ (2020a) Blood plasma phosphorylated-tau isoforms track CNS change in Alzheimer's disease. *J Exp Med* 217

Barthelemy NR, Li Y, Joseph-Mathurin N, Gordon BA, Hassenstab J, Benzinger TLS, Buckles V, Fagan AM, Perrin RJ, Goate AM *et al* (2020b) A soluble phosphorylated tau signature links tau, amyloid and the evolution of stages of dominantly inherited Alzheimer's disease. *Nat Med* 26: 398-407

Benarroch EE (2018) Glutamatergic synaptic plasticity and dysfunction in Alzheimer disease: Emerging mechanisms. *Neurology* 91: 125-132

Braak H, Alafuzoff I, Arzberger T, Kretzschmar H, Del Tredici K (2006) Staging of Alzheimer disease-associated neurofibrillary pathology using paraffin sections and immunocytochemistry. *Acta Neuropathol* 112: 389-404

Bramblett GT, Goedert M, Jakes R, Merrick SE, Trojanowski JQ, Lee VM (1993) Abnormal tau phosphorylation at Ser396 in Alzheimer's disease recapitulates development and contributes to reduced microtubule binding. *Neuron* 10: 1089-1099

Braun NJ, Yao KR, Alford PW, Liao D (2020) Mechanical injuries of neurons induce tau mislocalization to dendritic spines and tau-dependent synaptic dysfunction. *Proc Natl Acad Sci U S A* 117: 29069-29079

Bretteville A, Marcouiller F, Julien C, El Khoury NB, Petry FR, Poitras I, Mouginot D, Levesque G, Hebert SS, Planel E (2012) Hypothermia-induced hyperphosphorylation: a new model to study tau kinase inhibitors. *Sci Rep* 2: 480

Brion JP, Smith C, Couck AM, Gallo JM, Anderton BH (1993) Developmental changes in tau phosphorylation: fetal tau is transiently phosphorylated in a manner similar to paired helical filament-tau characteristic of Alzheimer's disease. *J Neurochem* 61: 2071-2080

Buss EW, Corbett NJ, Roberts JG, Ybarra N, Musial TF, Simkin D, Molina-Campos E, Oh KJ, Nielsen LL, Ayala GD *et al* (2021) Cognitive aging is associated with redistribution of synaptic weights in the hippocampus. *Proc Natl Acad Sci U S A* 118

Busse CS, Brodkin J, Tattersall D, Anderson JJ, Warren N, Tehrani L, Bristow LJ, Varney MA, Cosford ND (2004) The behavioral profile of the potent and selective mGlu5 receptor antagonist 3-[(2-methyl-1,3-thiazol-4-yl)ethynyl]pyridine (MTEP) in rodent models of anxiety. *Neuropsychopharmacology* 29: 1971-1979

Chang CW, Shao E, Mucke L (2021) Tau: Enabler of diverse brain disorders and target of rapidly evolving therapeutic strategies. *Science* 371

Collingridge GL, Peineau S, Howland JG, Wang YT (2010) Long-term depression in the CNS. *Nat Rev Neurosci* 11: 459-473

Connor SA, Wang YT (2016) A Place at the Table: LTD as a Mediator of Memory Genesis. *Neuroscientist* 22: 359-371

Debanne D, Gahwiler BH, Thompson SM (1998) Long-term synaptic plasticity between pairs of individual CA3 pyramidal cells in rat hippocampal slice cultures. *J Physiol* 507 (Pt 1): 237-247

Draffin JE, Sanchez-Castillo C, Fernandez-Rodrigo A, Sanchez-Saez X, Avila J, Wagner FF, Esteban JA (2021) GSK3alpha, not GSK3beta, drives hippocampal NMDAR-dependent LTD via tau-mediated spine anchoring. *EMBO J* 40: e105513

Driscoll I, Hamilton DA, Petropoulos H, Yeo RA, Brooks WM, Baumgartner RN, Sutherland RJ (2003) The aging hippocampus: cognitive, biochemical and structural findings. *Cereb Cortex* 13: 1344-1351

Goedert M, Jakes R, Crowther RA, Six J, Lubke U, Vandermeeren M, Cras P,

536 Trojanowski JQ, Lee VM (1993) The abnormal phosphorylation of tau protein at
537 Ser-202 in Alzheimer disease recapitulates phosphorylation during development.
538 *Proc Natl Acad Sci U S A* 90: 5066-5070

539 Gratuze M, El Khoury NB, Turgeon A, Julien C, Marcouiller F, Morin F, Whittington
540 RA, Marette A, Calon F, Planel E (2017) Tau hyperphosphorylation in the brain of
541 ob/ob mice is due to hypothermia: Importance of thermoregulation in linking
542 diabetes and Alzheimer's disease. *Neurobiol Dis* 98: 1-8

543 Hansson O (2021) Biomarkers for neurodegenerative diseases. *Nat Med* 27: 954-963

544 Hefti MM, Kim S, Bell AJ, Betters RK, Fiock KL, Iida MA, Smalley ME, Farrell K,
545 Fowkes ME, Crary JF (2019) Tau Phosphorylation and Aggregation in the
546 Developing Human Brain. *J Neuropathol Exp Neurol* 78: 930-938

547 Hou Y, Dan X, Babbar M, Wei Y, Hasselbalch SG, Croteau DL, Bohr VA (2019)
548 Ageing as a risk factor for neurodegenerative disease. *Nat Rev Neurol* 15: 565-581

549 Hu NW, Nicoll AJ, Zhang D, Mably AJ, O'Malley T, Purro SA, Terry C, Collinge J,
550 Walsh DM, Rowan MJ (2014) mGlu5 receptors and cellular prion protein mediate
551 amyloid-beta-facilitated synaptic long-term depression in vivo. *Nat Commun* 5:
552 3374

553 Hu Z, Yu P, Zhang Y, Yang Y, Zhu M, Qin S, Xu JT, Duan D, Wu Y, Wang D *et al*
554 (2022) Inhibition of the ISR abrogates mGluR5-dependent long-term depression
555 and spatial memory deficits in a rat model of Alzheimer's disease. *Transl*
556 *Psychiatry* 12: 96

557 Ianov L, De Both M, Chawla MK, Rani A, Kennedy AJ, Piras I, Day JJ, Siniard A,
558 Kumar A, Sweatt JD *et al* (2017) Hippocampal Transcriptomic Profiles: Subfield
559 Vulnerability to Age and Cognitive Impairment. *Front Aging Neurosci* 9: 383

560 Karikari TK, Pascoal TA, Ashton NJ, Janelidze S, Benedet AL, Rodriguez JL,
561 Chamoun M, Savard M, Kang MS, Therriault J *et al* (2020) Blood phosphorylated
562 tau 181 as a biomarker for Alzheimer's disease: a diagnostic performance and
563 prediction modelling study using data from four prospective cohorts. *Lancet*
564 *Neurol* 19: 422-433

565 Kimura T, Whitcomb DJ, Jo J, Regan P, Piers T, Heo S, Brown C, Hashikawa T,
566 Murayama M, Seok H *et al* (2014) Microtubule-associated protein tau is essential
567 for long-term depression in the hippocampus. *Philos Trans R Soc Lond B Biol Sci*
568 369: 20130144

569 Kotecha SA, Jackson MF, Al-Mahrouki A, Roder JC, Orser BA, MacDonald JF (2003)
570 Co-stimulation of mGluR5 and N-methyl-D-aspartate receptors is required for
571 potentiation of excitatory synaptic transmission in hippocampal neurons. *J Biol*
572 *Chem* 278: 27742-27749

573 Krukowski K, Nolan A, Frias ES, Boone M, Ureta G, Grue K, Paladini MS,

574 Elizarraras E, Delgado L, Bernales S *et al* (2020) Small molecule cognitive
575 enhancer reverses age-related memory decline in mice. *Elife* 9

576 Li S, Hong S, Shepardson NE, Walsh DM, Shankar GM, Selkoe D (2009) Soluble
577 oligomers of amyloid Beta protein facilitate hippocampal long-term depression by
578 disrupting neuronal glutamate uptake. *Neuron* 62: 788-801

579 Liu DD, Yang Q, Li ST (2013) Activation of extrasynaptic NMDA receptors induces
580 LTD in rat hippocampal CA1 neurons. *Brain Res Bull* 93: 10-16

581 Liu F, Iqbal K, Grundke-Iqbal I, Gong CX (2002) Involvement of aberrant
582 glycosylation in phosphorylation of tau by cdk5 and GSK-3beta. *FEBS Lett* 530:
583 209-214

584 Livingston G, Huntley J, Sommerlad A, Ames D, Ballard C, Banerjee S, Brayne C,
585 Burns A, Cohen-Mansfield J, Cooper C *et al* (2020) Dementia prevention,
586 intervention, and care: 2020 report of the Lancet Commission. *Lancet* 396:
587 413-446

588 Lujan R, Nusser Z, Roberts JD, Shigemoto R, Somogyi P (1996) Perisynaptic location
589 of metabotropic glutamate receptors mGluR1 and mGluR5 on dendrites and
590 dendritic spines in the rat hippocampus. *Eur J Neurosci* 8: 1488-1500

591 Lujan R, Roberts JD, Shigemoto R, Ohishi H, Somogyi P (1997) Differential plasma
592 membrane distribution of metabotropic glutamate receptors mGluR1 alpha,
593 mGluR2 and mGluR5, relative to neurotransmitter release sites. *J Chem Neuroanat*
594 13: 219-241

595 Luscher C, Huber KM (2010) Group 1 mGluR-dependent synaptic long-term
596 depression: mechanisms and implications for circuitry and disease. *Neuron* 65:
597 445-459

598 Magee JC, Grienberger C (2020) Synaptic Plasticity Forms and Functions. *Annu Rev*
599 *Neurosci* 43: 95-117

600 McCamphill PK, Stoppel LJ, Senter RK, Lewis MC, Heynen AJ, Stoppel DC, Sridhar
601 V, Collins KA, Shi X, Pan JQ *et al* (2020) Selective inhibition of glycogen
602 synthase kinase 3alpha corrects pathophysiology in a mouse model of fragile X
603 syndrome. *Sci Transl Med* 12

604 McKiernan EC, Marrone DF (2017) CA1 pyramidal cells have diverse biophysical
605 properties, affected by development, experience, and aging. *PeerJ* 5: e3836

606 Mishiba T, Tanaka M, Mita N, He X, Sasamoto K, Itohara S, Ohshima T (2014)
607 Cdk5/p35 functions as a crucial regulator of spatial learning and memory. *Mol*
608 *Brain* 7: 82

609 Nies SH, Takahashi H, Herber CS, Huttner A, Chase A, Strittmatter SM (2021)
610 Spreading of Alzheimer tau seeds is enhanced by aging and template matching
611 with limited impact of amyloid-beta. *J Biol Chem* 297: 101159

O'Connor A, Karikari TK, Poole T, Ashton NJ, Lantero Rodriguez J, Khatun A, Swift I, Heslegrave AJ, Abel E, Chung E *et al* (2020) Plasma phospho-tau181 in presymptomatic and symptomatic familial Alzheimer's disease: a longitudinal cohort study. *Mol Psychiatry*

O'Riordan KJ, Hu NW, Rowan MJ (2018a) Ass Facilitates LTD at Schaffer Collateral Synapses Preferentially in the Left Hippocampus. *Cell Rep* 22: 2053-2065

O'Riordan KJ, Hu NW, Rowan MJ (2018b) Physiological activation of mGlu5 receptors supports the ion channel function of NMDA receptors in hippocampal LTD induction in vivo. *Sci Rep* 8: 4391

Ondrejcak T, Hu NW, Qi Y, Klyubin I, Corbett GT, Fraser G, Perkinton MS, Walsh DM, Billinton A, Rowan MJ (2019) Soluble tau aggregates inhibit synaptic long-term depression and amyloid beta-facilitated LTD in vivo. *Neurobiol Dis* 127: 582-590

Palmqvist S, Tideman P, Cullen N, Zetterberg H, Blennow K, Alzheimer's Disease Neuroimaging I, Dage JL, Stomrud E, Janelidze S, Mattsson-Carlgren N *et al* (2021) Prediction of future Alzheimer's disease dementia using plasma phospho-tau combined with other accessible measures. *Nat Med* 27: 1034-1042

Papouin T, Ladepeche L, Ruel J, Sacchi S, Labasque M, Hanini M, Groc L, Pollegioni L, Mothet JP, Oliet SH (2012) Synaptic and extrasynaptic NMDA receptors are gated by different endogenous coagonists. *Cell* 150: 633-646

Peineau S, Taghibiglou C, Bradley C, Wong TP, Liu L, Lu J, Lo E, Wu D, Saule E, Bouschet T *et al* (2007) LTP inhibits LTD in the hippocampus via regulation of GSK3beta. *Neuron* 53: 703-717

Percie du Sert N, Hurst V, Ahluwalia A, Alam S, Avey MT, Baker M, Browne WJ, Clark A, Cuthill IC, Dirnagl U *et al* (2020) The ARRIVE guidelines 2.0: Updated guidelines for reporting animal research. *PLoS Biol* 18: e3000410

Planel E, Miyasaka T, Launey T, Chui DH, Tanemura K, Sato S, Murayama O, Ishiguro K, Tatebayashi Y, Takashima A (2004) Alterations in glucose metabolism induce hypothermia leading to tau hyperphosphorylation through differential inhibition of kinase and phosphatase activities: implications for Alzheimer's disease. *J Neurosci* 24: 2401-2411

Potier B, Billard JM, Riviere S, Sinet PM, Denis I, Champeil-Potokar G, Grintal B, Jouvenceau A, Kollen M, Dutar P (2010) Reduction in glutamate uptake is associated with extrasynaptic NMDA and metabotropic glutamate receptor activation at the hippocampal CA1 synapse of aged rats. *Aging Cell* 9: 722-735

Regan P, Piers T, Yi JH, Kim DH, Huh S, Park SJ, Ryu JH, Whitcomb DJ, Cho K (2015) Tau phosphorylation at serine 396 residue is required for hippocampal LTD. *J Neurosci* 35: 4804-4812

650 Sarantis K, Tsiamaki E, Kouvaros S, Papatheodoropoulos C, Angelatou F (2015)
651 Adenosine A(2)A receptors permit mGluR5-evoked tyrosine phosphorylation of
652 NR2B (Tyr1472) in rat hippocampus: a possible key mechanism in NMDA
653 receptor modulation. *J Neurochem* 135: 714-726

654 Sato C, Barthelemy NR, Mawuenyega KG, Patterson BW, Gordon BA,
655 Jockel-Balsarotti J, Sullivan M, Crisp MJ, Kasten T, Kirmess KM *et al* (2018) Tau
656 Kinetics in Neurons and the Human Central Nervous System. *Neuron* 97:
657 1284-1298 e1287

658 Sindou P, Lesort M, Couratier P, Yardin C, Esclaire F, Hugon J (1994) Glutamate
659 increases tau phosphorylation in primary neuronal cultures from fetal rat cerebral
660 cortex. *Brain Res* 646: 124-128

661 Sun XY, Tuo QZ, Liuyang ZY, Xie AJ, Feng XL, Yan X, Qiu M, Li S, Wang XL, Cao
662 FY *et al* (2016) Extrasynaptic NMDA receptor-induced tau overexpression
663 mediates neuronal death through suppressing survival signaling ERK
664 phosphorylation. *Cell Death Dis* 7: e2449

665 Tackenberg C, Grinschgl S, Trutzel A, Santuccione AC, Frey MC, Konietzko U,
666 Grimm J, Brandt R, Nitsch RM (2013) NMDA receptor subunit composition
667 determines beta-amyloid-induced neurodegeneration and synaptic loss. *Cell Death*
668 *Dis* 4: e608

669 Taylor HBC, Emptage NJ, Jeans AF (2021) Long-term depression links amyloid-beta
670 to the pathological hyperphosphorylation of tau. *Cell Rep* 36: 109638

671 Teunissen CE, Verberk IMW, Thijssen EH, Vermunt L, Hansson O, Zetterberg H, van
672 der Flier WM, Mielke MM, Del Campo M (2022) Blood-based biomarkers for
673 Alzheimer's disease: towards clinical implementation. *Lancet Neurol* 21: 66-77

674 Veldsman M, Nobis L, Alfaro-Almagro F, Manohar S, Husain M (2021) The human
675 hippocampus and its subfield volumes across age, sex and APOE e4 status. *Brain*
676 *Commun* 3: fcaa219

677 Vieira M, Yong XLH, Roche KW, Anggono V (2020) Regulation of NMDA glutamate
678 receptor functions by the GluN2 subunits. *J Neurochem*

679 Wegmann S, Bennett RE, Delorme L, Robbins AB, Hu M, McKenzie D, Kirk MJ,
680 Schiantarelli J, Tunio N, Amaral AC *et al* (2019) Experimental evidence for the age
681 dependence of tau protein spread in the brain. *Sci Adv* 5: eaaw6404

682 Wegmann S, Biernat J, Mandelkow E (2021) A current view on Tau protein
683 phosphorylation in Alzheimer's disease. *Curr Opin Neurobiol* 69: 131-138

684 Wesseling H, Mair W, Kumar M, Schlaffner CN, Tang S, Beerepoot P, Fatou B, Guise
685 AJ, Cheng L, Takeda S *et al* (2020) Tau PTM Profiles Identify Patient
686 Heterogeneity and Stages of Alzheimer's Disease. *Cell* 183: 1699-1713 e1613

687 Wu JW, Hussaini SA, Bastille IM, Rodriguez GA, Mrejeru A, Rilett K, Sanders DW,

688 Cook C, Fu H, Boonen RA *et al* (2016) Neuronal activity enhances tau propagation
689 and tau pathology in vivo. *Nat Neurosci* 19: 1085-1092

690 Yu Y, Run X, Liang Z, Li Y, Liu F, Liu Y, Iqbal K, Grundke-Iqbal I, Gong CX (2009)
691 Developmental regulation of tau phosphorylation, tau kinases, and tau
692 phosphatases. *J Neurochem* 108: 1480-1494

693

694

695 **Supporting Information Listing**

696 Table S1: Antibodies used in this study

697 Figure S1-11 and legends

698

Figure legends

Figure 1 LFS promotes p-Tau181 in an age-dependent manner in live rats. (a) Schematic of the field EPSPs recording configuration in CA1 stratum radiatum (REC) overlaid with a schematic of a bipolar stimulation electrode (STIM) for Schaffer collateral axon fibers (black) in ipsilateral hemisphere. Additional excitatory projections from CA3 include local recurrent connections (blue) of CA3 pyramidal cells onto other CA3 pyramidal cells, and the back projection (pink) of CA3 pyramidal neurons to the dentate gyrus (DG). (b) Application of LFS (horizontal bar, LFS-900; 900 pulses at 1Hz) induced robust LTD at CA3-CA1 synapses in anaesthetized rats at two different ages (2-3-month, and 17-18-month). Calibration bars: vertical, 2 mV; horizontal, 10 ms. (c) Summarized EPSP amplitude 30 min post LFS. The EPSP decreased to 63.8 ± 7.8% in 2-3-month-old rats (n = 5, $P = 0.0147$ compared with Pre), and 62.4 ± 3.4% in 17-18-month-old rats (n = 7, $P < 0.0001$ compared with Pre) respectively; paired *t* test. The amplitude of LTD is comparable in both groups (two-way ANOVA, age, F (1, 10) = 0.09427, $P = 0.7651$). (d) The upper panel shows p-Tau181 (red) immunofluorescent staining in dorsal hippocampus (Scale bar: 200 μm), CA1, CA3, and hilus of DG (scale bars: 50 μm) from 2-3-month-old rats. The corresponding statistical results compared with contralateral side are displayed in the lower panel. The expression level of p-Tau181 was not affected by LFS in dorsal hippocampus ($P = 0.4611$), CA1 ($P = 0.3792$), CA3 ($P = 0.6842$), and DG ($P = 0.1953$); paired *t* test. (e) Immunofluorescent staining of

720 p-Tau181 (red) in ipsilateral dorsal hippocampus, CA1, CA3, and DG from
721 17-18-month-old rats. LTD induction by LFS significantly enhanced the level of
722 p-Tau181 in dorsal hippocampus ($P < 0.0001$), CA1 ($P = 0.0220$), CA3 ($P = 0.0059$),
723 and DG ($P = 0.0202$); paired *t* test. Values are mean ± s.e.m.

724 **Figure 2 LFS promotes p-Tau217 in an age-dependent manner in live rats.** (a)
725 The upper panel shows immunofluorescent staining of p-Tau217 (red) in dorsal
726 hippocampus (Scale bar: 200 μm), CA1, CA3, and DG (scale bars: 50 μm) from
727 2-3-month-old rats. The corresponding mean fluorescence intensities were
728 summarized in the lower panel. LFS did not affect the expression level of p-Tau217 in
729 dorsal hippocampus ($P = 0.3820$), CA1 ($P = 0.4488$), CA3 ($P = 0.3409$), and DG ($P =$
730 0.1567); paired *t* test. (b) Immunofluorescent staining of p-Tau217 (red) in dorsal
731 hippocampus, CA1, CA3, and DG from 17-18-month-old rats. LFS ipsilaterally
732 enhanced the level of p-Tau217 in dorsal hippocampus ($P < 0.0019$), CA1 ($P =$
733 0.0153), CA3 ($P = 0.0003$), and DG ($P = 0.0251$); paired *t* test. Values are mean ±
734 s.e.m.

735 **Figure 3 LFS enhances p-Tau181 and p-Tau217 in aged rats.** (a) Application of
736 LFS-900 induced robust LTD at CA3-CA1 synapses in anaesthetized
737 17-18-month-old rats. Calibration bars: vertical, 2 mV; horizontal, 10 ms. (b)
738 Summarized EPSP amplitude 30 min post LFS. The EPSP decreased to 54.8 ± 10.2%
739 (n = 5, $P = 0.0110$ compared with Pre, paired *t*). (c) Left panels show representative
740 blotting band of p-Tau181 and total tau (Tau5) in the hippocampus of age-matched

naïve control group and the experimental group either contralateral or ipsilateral to LFS. Statistical results of p-Tau181 over total tau was quantified and normalized to naïve control (n = 5 per group, ipsilateral vs naïve, $P = 0.0292$; contralateral vs naïve, $P = 0.5075$; contralateral vs ipsilateral, $P = 0.4022$; one-way ANOVA-Bonferroni). (d) Left panels show representative blotting band of p-Tau217 and total tau (tau5) in age-matched naïve control group, contralateral hippocampus, and ipsilaterally stimulated hippocampus. Statistical results of p-Tau217 over total tau was quantified and normalized to naïve control (n = 5 per group, ipsilateral vs naïve, $P = 0.0049$; contralateral vs naïve, $P = 0.0979$; contralateral vs ipsilateral, $P = 0.3905$; one-way ANOVA-Bonferroni). Values are mean ± s.e.m.

Figure 4 Antagonists of either NMDA receptors or mGluR5 prevent the elevation of both p-Tau181 and p-Tau217 induced by LFS in aged rats. (**a)** Systemic injection of competitive NMDAR antagonist CPP (10 mg/kg, i.p.) alone 1 h prior to the application of LFS did not affect LTD induction in 17-18-month-old rats. Similarly, intraperitoneal injection of the mGluR5 negative allosteric modulator MTEP (3 mg/kg) alone 1 h did not affect LTD induction by LFS 1 h later in 17-18m old rats. Calibration bars: vertical, 2 mV; horizontal, 10 ms. (**b)** Summary of the mean EPSP amplitude pre and post -LFS. The EPSP decreased to 70.2 ± 2.5% (n = 6, $P <$ 0.0001 compared with pre, paired *t* test) and 79.6 ± 3.7% (n = 5, $P = 0.0068$ compared with pre, paired *t* test) 30 min post-LFS in CPP or MTEP treated rats respectively (two-way RM ANOVA, Treatment $F_{1, 9} = 6.999$, $P = 0.0267$). (**c)** The upper panel

762 shows the fluorescent images of p-Tau181 labeling (red) and the lower panel displays
763 the corresponding statistical results in CPP-treated 17-18-month-old rats (Scale bar =
764 200 μm in dorsal hippocampus; scale bars = 50 μm in CA1, CA3 and DG regions).
765 LTD induction by LFS did not affect the level of p-Tau181 in dorsal dorsal
766 hippocampus (P = 0.1218), CA3 (P = 0.6147), and DG (P = 0.0578) except for CA1
767 region (P = 0.0353); paired t test. (**d)** The upper panel shows the fluorescent images
768 of p-Tau217 labeling (red) and the corresponding statistical results are displayed in
769 the lower panel in CPP-treated 17-18-month-old rats. No significant difference was
770 found in p-Tau217 level compared with that in contralateral dorsal hippocampus (P =
771 0.8075), CA1 (P = 0.0920), CA3 (P = 0.5811), and DG (P = 0.7041); paired t test. (**e)**
772 In MTEP-treated aged rats, LFS failed to promote the level of p-Tau181 (red as
773 showed in the upper panel). Summarized mean fluorescence intensities (fold to
774 contralateral) in dorsal hippocampus (P = 0.9154), CA1 (P = 0.3161), CA3 (P =
775 0.1839), and DG (P = 0.8417); paired t test. (**f)** MTEP treatment also prevented the
776 enhancement of p-Tau217 by LFS in aged rats. The upper panel showed the
777 fluorescent images of p-Tau217 (red). The corresponding statistical results were
778 displayed in the lower panel and no significant difference was found in dorsal
779 hippocampus (P = 0.7702), CA1 (P = 0.1598), CA3 (P = 0.2262), and DG (P =
780 0.5311); paired t test. Values are mean ± s.e.m.

781 **Figure 5 ISRIB blocks LFS-induced enhancement of p-Tau181 and p-Tau217 in**
782 **aged rats.** (a) Experimental paradigm for ISRIB injection and electrophysiology

783 experiments. ISRIB (2.5 mg/kg, i.p.) was systemically injected for 3 days and *in vivo*
784 electrophysiology experiments were performed 18 days after the last injection. (b)
785 LFS induced robust LTD in ISRIB-treated aged rats. Calibration bars: vertical, 2 mV;
786 horizontal, 10 ms. (c) The EPSP decreased to 81.8 ± 2.7% at 30 min post LFS (n = 4,
787 $P = 0.0211$ compared with pre, paired *t* test). (d) Treatment of ISRIB completely
788 prevented the increase of p-Tau181 induced by LFS in aged rats. The upper panel
789 showed the fluorescent images of p-Tau181 labeling (red). As summarized in the
790 lower panel, no significant difference was found in the dorsal hippocampus ($P =$
791 0.0579), CA1 ($P = 0.7006$), CA3 ($P = 0.0715$), and DG ($P = 0.2696$); paired *t* test. (e)
792 Treatment of ISRIB also successfully blocked the enhancement of p-Tau217 induced
793 by LFS in aged rats. The upper panel showed the fluorescent images of p-Tau217
794 labeling (red). Summarized statistic results in the lower panel displayed no significant
795 difference in all regions including dorsal hippocampus ($P = 0.1185$), CA1 ($P =$
796 0.9049), CA3 ($P = 0.9172$), and DG ($P = 0.6636$); paired *t* test. Scale bar = 200 μm in
797 hippocampus, scale bar = 50 μm in CA1, CA3 and DG regions. Values are mean ±
798 s.e.m.

799

Figures

Fig 1

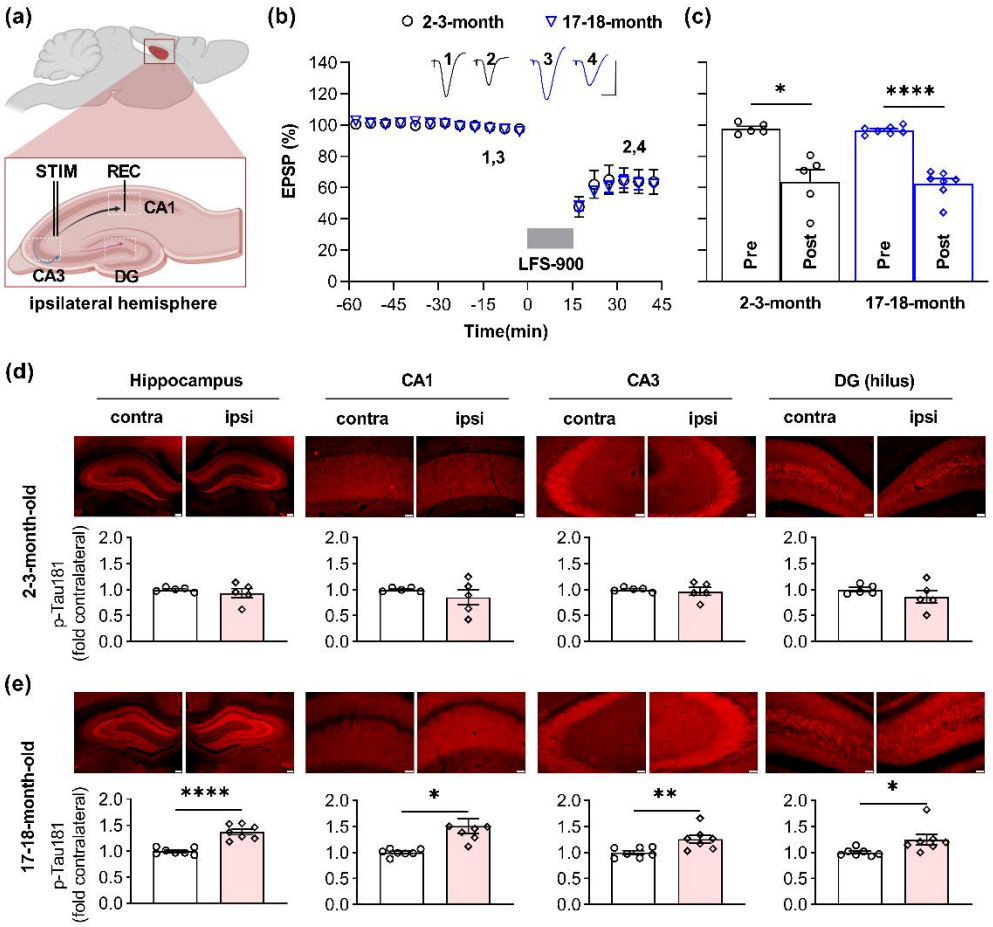

Fig 2

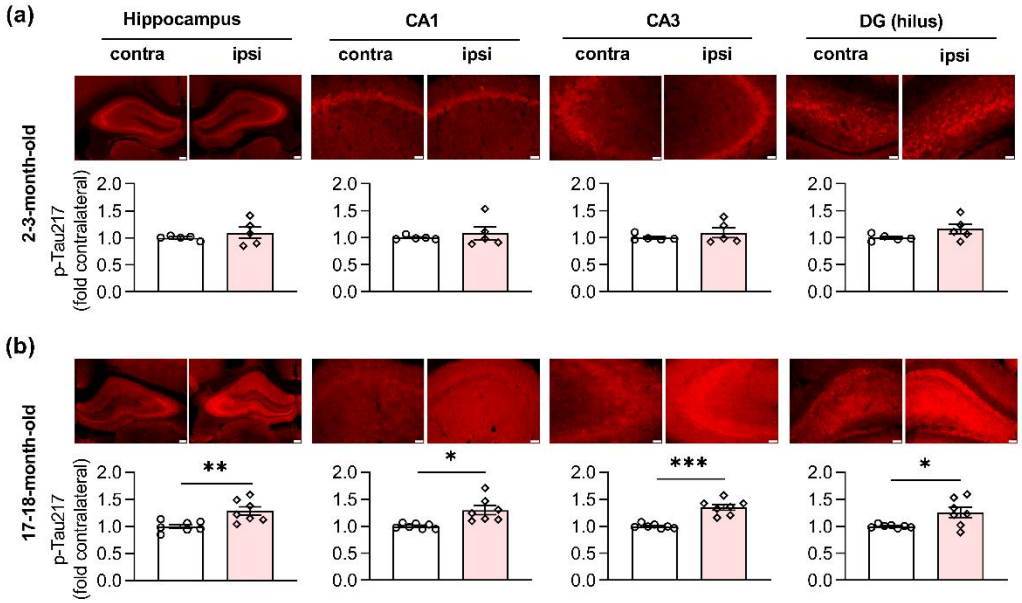

803

804

Fig 3

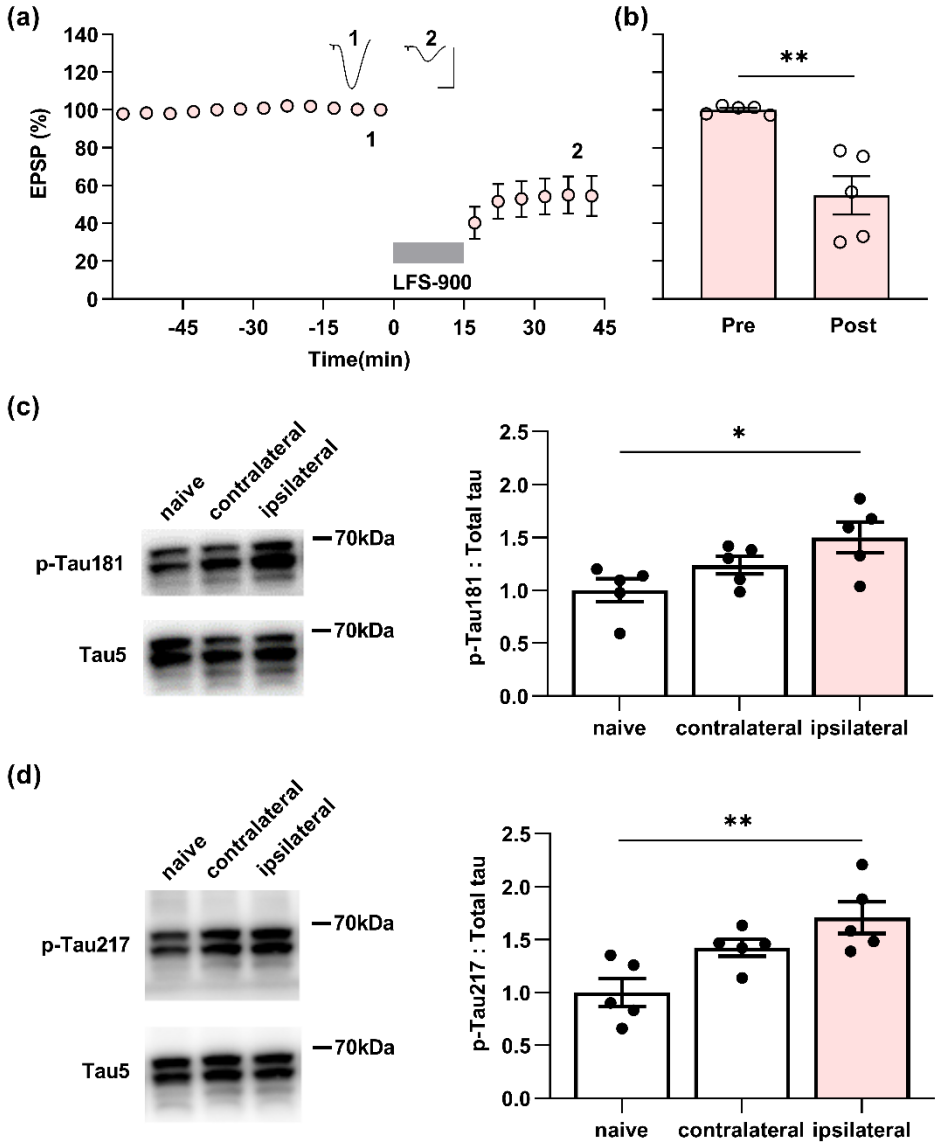

805
806

Fig 4

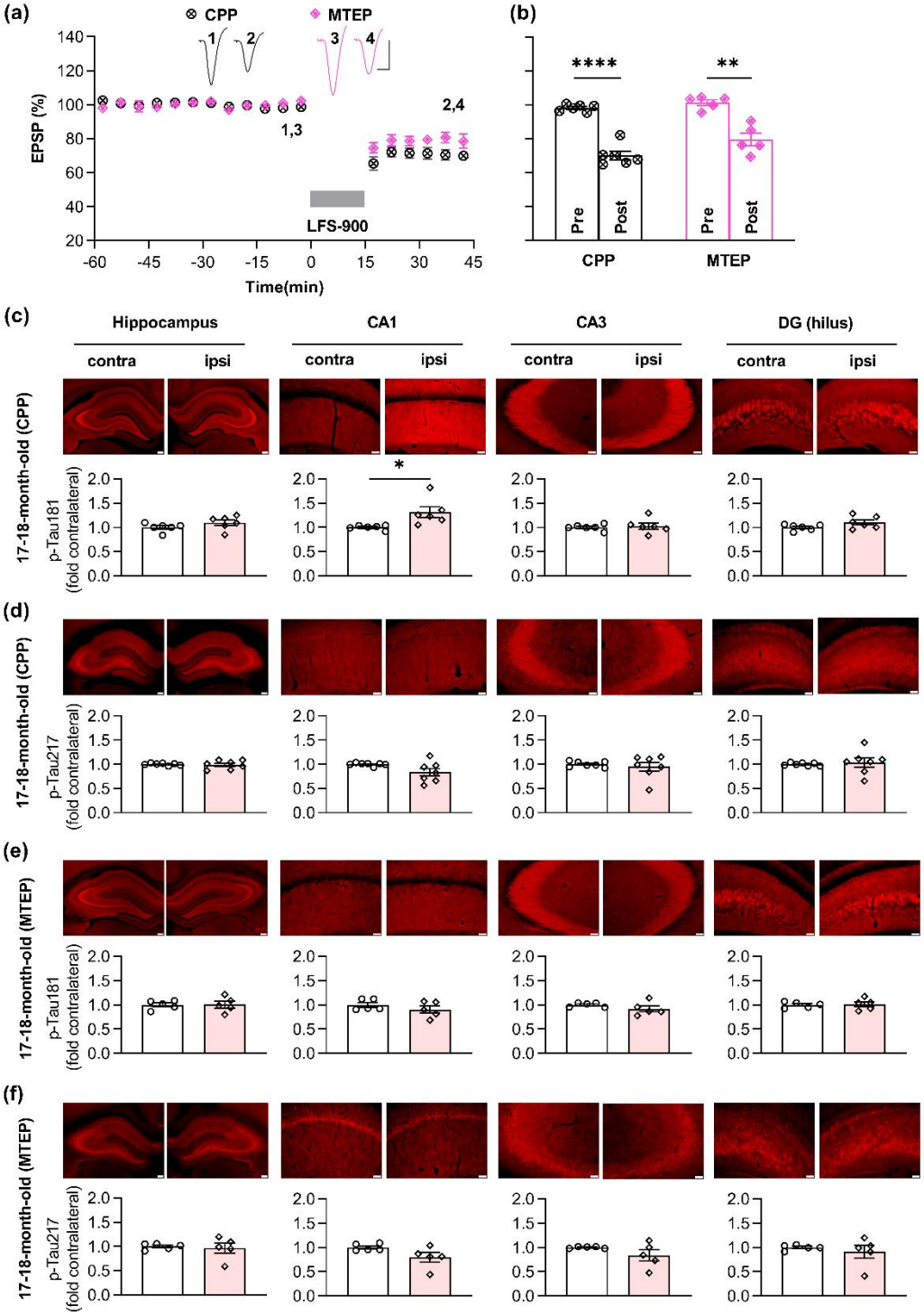

807

808

Fig 5

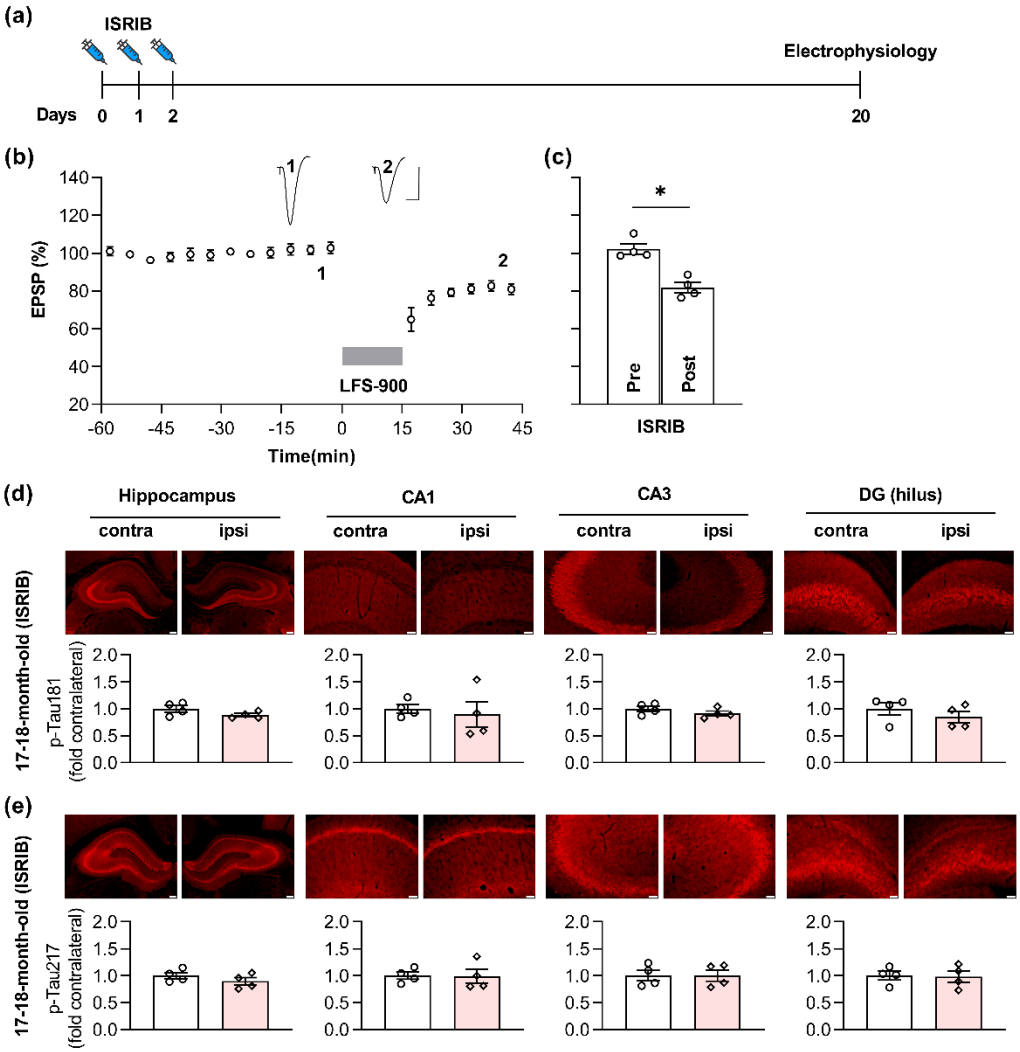

809